# Integral Equation Theory for the Interactions between Passivated Nanocrystals in Supercritical Fluids: Solvophobic and Solvophilic Cases

**Eran Rabani*,† and S.A. Egorov‡**

*School of Chemistry, Tel Aviv University, Tel Aviv 69978, Israel, and Department of Chemistry, University of Virginia, Charlottesville, Virginia 22903*

*Received: February 26, 2002; In Final Form: April 30, 2002*

A study of the interactions between nanocrystals in supercritical fluids for the solvophobic and solvophilic cases is presented. The model for the nanocrystal consists of a highly polarizable core and a passivation layer, both of which are uniformly composed of Lennard-Jones particles. A nonlocal integral equation theory is applied to study the excess and total potential of mean force between the nanocrystals. The effects of solvent density, and thickness and density of passivation layer, on the total potential of mean force and on solubility of nanocrystals in solutions is discussed. Important differences observed between solvophobic and solvophilic cases are analyzed in terms of the local solvent density profile around the nanocrystals. Interesting characteristic features, such as the disappearance of anomalous behavior previously reported by us for nonpassivated attractive solutes, are predicted. Certain qualitative feature observed in experimental studies of nanocrystal interactions in supercritical solvents are well reproduced within the model.

## I. Introduction

Synthetic preparation of nanocrystals using controlled precipitation techniques typically involves dissolution of metallic or semiconductor nanocrystals, which are coated by chemically adsorbed organic ligands.[1−12] These metallic or semiconductor nanocrystals self-assemble to form 2D superlattices when the solvent is evaporated, provided that the size distribution of the nanocrystals is sufficiently narrow.[12−24] One of the key factors that govern the controlled precipitation and self-assembly processes is the solvent-mediated interaction potential between the nanocrystals.[16]

Numerous studies of suspensions of small colloidal particles[25−32] and of reverse micelles[33−35] have indicated that the solvent-mediated particle−particle interaction potential has a significantly richer structure than the potential obtained from the continuum model of the solvent, where the interactions are described by the Hamaker potential,[36] and the effect of the solvent is taken into account by scaling the Hamaker constant.[37] Whereas the same is also true for nanocrystals,[38,39] the detailed features of the solvent-mediated interaction potential between nanocrystals and its dependence on the solvent properties can be expected to differ significantly from those of colloidal particles and reverse micelles because the nanocrystals are typically neutral and have a highly polarizable metallic or inorganic core that is passivated with organic ligands.

Given the significance of controlled precipitation and self-assembly of nanocrystals, it is surprising that the study of the interaction potential between solvated nanocrystals has received very little attention.[38−40] In a recent set of papers[38,39] we have discussed the effects of the solvent on the interaction potential between two nanocrystals under "normal" liquid conditions. The model for a nanocrystal consisting of a central core of radius $R_c$ surrounded by a spherical shell of thickness $R_p - R_c$ that represents the passivation layer (see Figure 1) was employed. The nanocrystal core and passivation shell were uniformly composed of Lennard-Jones (LJ) particles. By tuning the degree of solvophobicity through an independent solvent-passivation interaction strength parameter, it was found that for the solvophobic case the nanocrystal−nanocrystal interaction potential is strongly enhanced by the solvent and solvation of the nanocrystals is not favorable, whereas the opposite is true for the solvophilic case.[38] In addition, it was shown that it is possible to vary the interaction strength between nanocrystals in dense liquids by an amount comparable to the thermal energy by adding small amounts of cosolvent with respect to which the nanocrystals are solvophobic.[39]

There are still numerous open question regarding the effects of solvent density and the thickness and density of the passivation layer on the solvent-mediated interaction potential between nanocrystals. In particular, how would the interactions between the nanocrystals change upon reducing the solvent density to the supercritical regime in the solvophobic and solvophilic cases? Studies of the solvent-mediated interaction potential between Lennard-Jones particles in Lennard-Jones solvents have revealed an anomalous density dependence for the solvent-mediated interaction potential.[41−43] In view of these findings, one can ask whether nanocrystals would show similar anomalous behavior and how supercritical solvents can be used to control the degree of solubility of both solvophobic and solvophilic nanocrystals?

Recent experimental results by Johnston, Korgel, and coworkers have demonstrated that upon changing the density of the solvent one can vary the degree of nanocrystal solubility, thereby increasing size selectivity.[44−46] Furthermore, the nanocrystals can be dissolved in various solvents, including supercritical water, by reducing the solvent density.[47] In this paper, we extend our study of the solvent-mediated interaction potential between nanocrystals to lower- and medium-density regimes along a supercritical isotherm. The study is based on a continuum model for the nanocrystal core and passivation layer

* Corresponding author. E-mail: rabani@tau.ac.il.
† Tel Aviv University.
‡ University of Virginia.

10.1021/jp025693f CCC: $22.00 
Published on Web 05/31/2002

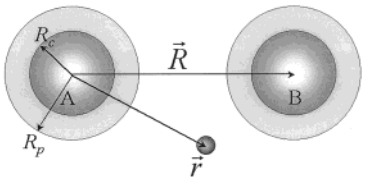


**Figure 1.** Sketch of the model used to describe the passivated nanocrystals. $R_c$ and $R_p$ are the radii of the core and passivation layer, respectively, and **R** is the position vector of nanocrystal B, given that nanocrystal A is at the origin. The position vector of a representative solvent molecule is given by **r**.

combined with a molecular model for the solvent. The molecular model of the solvent is especially warranted for supercritical solvents, which are characterized by significant density inhomogeneities that cannot be captured within the continuum treatment.[48,49] We study the effects of solvent density, thickness and density of the passivation layer, solvent-passivation interaction strength, and size of the particles on the solvent-mediated interaction potentials for solvophobic and solvophilic nanocrystals. Furthermore, the anomalous behavior observed in the solvent-mediated interaction potential of Lennard-Jones particles in supercritical fluids and possible ways to dissolve solvophobic nanocrystals are discussed.

The paper is organized as follows: In section II, the microscopic models for the passivated nanocrystal and for the solvent are specified. For completeness, the nonlocal integral equation used to study the solvent-mediated interaction potential between the nanocrystals is described. In sections III and IV, extensive model calculations of the total and excess potentials of mean force between nanocrystals for a wide range of solvent thermodynamic conditions and model parameters for both the solvophobic and the solvophilic cases are presented. The results are analyzed in terms of the local solvent density profile induced by the two nanocrystals. A summary of the results and conclusions is given in section V.

## II. Model and Theory

The model for a nanocrystal consists of a central core of radius $R_c$ surrounded by a spherical shell of thickness $R_p - R_c$ that represents the passivation layer (see Figure 1). The nanocrystal core and passivation shell are uniformly composed of LJ particles with number densities $\rho_c$ and $\rho_p$, respectively. The solvent is modeled as a LJ fluid with a number density $\rho_s$ and LJ parameters $\epsilon_s$ and $\sigma_s$. The LJ parameters for the atoms comprising the core and the passivation shell of the nanocrystal are $\epsilon_c$, $\sigma_c$ and $\epsilon_p$, $\sigma_p$, respectively. The standard combining rules for the cross terms of the solvent−nanocrystal parameters $\epsilon_{sc} = \sqrt{\epsilon_s\epsilon_c}$and $\sigma_{sc} = {}^1/_2(\sigma_s + \sigma_c)$ and for $\sigma_{sp} = {}^1/_2(\sigma_s + \sigma_p)$ are used, whereas $\epsilon_{sp}$ (the coupling strength between the solvent and the passivation shell) is taken to be an independent parameter (see the discussion below). Similarly, the standard combing rules for the cross terms of the core-passivation parameters $\epsilon_{cp} = \sqrt{\epsilon_c\epsilon_p}$ and $\sigma_{cp} = {}^1/_2(\sigma_c + \sigma_p)$ are used.

The analytic forms for solvent−nanocrystal ($u_{sn}(r)$) and nanocrystal−nanocrystal ($u_{nn}(r)$) direct interaction potentials are obtained by integrating the individual LJ interactions over the volume of the corresponding spheres.[50] The result for the solvent−nanocrystal interaction potential is given by

$$u_{sn}(r) = u_c(r, R_c) + u_p(r, R_p) - u_p(r, R_c) \tag{1}$$

where

$$u_i(r, R_i) = C_{12}^i I_{12}(r, R_i) - C_6^i I_6(r, R_i) \tag{2}$$

and $R_i$ is the radius of sphere $i = c, p$, $C_{12}^i = 4\epsilon_{si}\sigma_{si}^{12}\rho_i$, and $C_6^i = 4\epsilon_{si}\sigma_{si}^6\rho_i$. In eq 2, $I_{12}(r, R_i)$ and $I_6(r, R_i)$ are given by

$$I_{12}(r, R_i) = \frac{4\pi}{45}R_i^3[15r^6 + 63r^4R_i^2 + 45r^2R_i^4 + 5R_i^6](r^2 - R_i^2)^{-9} \tag{3}$$

and

$$I_6(r, R_i) = \frac{4\pi}{3}R_i^3(r^2 - R_i^2)^{-3} \tag{4}$$

respectively.

Similarly, the nanocrystal−nanocrystal direct interaction potential can be derived and is given by

$$u_{nn}(r) = u_{cc}(r, R_c^A, R_c^B) + u_{pp}(r, R_p^A, R_p^B) + u_{pp}(r, R_c^A, R_c^B) + u_{cp}(r, R_c^A, R_p^B) + u_{pc}(r, R_p^A, R_c^B) - u_{cp}(r, R_c^A, R_c^B) - u_{pc}(r, R_c^A, R_c^B) - u_{pp}(r, R_p^A, R_c^B) - u_{pp}(r, R_c^A, R_p^B) \tag{5}$$

where $u_{ij}(r, R_A, R_B)$ $(i, j = c, p)$ is given by

$$u_{ij}(r, R_A, R_B) = C_{12}^{ij}V_{12}(r, R_A, R_B) - C_6^{ij}V_6(r, R_A, R_B) \tag{6}$$

and the coefficients $C_{12}^{ij} = 4\epsilon_{ij}\sigma_{ij}^{12}\rho_i\rho_j$ and $C_6^{ij} = 4\epsilon_{ij}\sigma_{ij}^6\rho_i\rho_j$ were obtained from standard combining rules. The short-range repulsion term $V_{12}(r, R_A, R_B)$ is given by

$$V_{12}(r, R_A, R_B) = \frac{16}{4725}\pi^2R_A^3R_B^3\sum_{n=0}^{8}\frac{P_{16-2n}(R_A, R_B)r^{2n}}{([(r + R_A)^2 - R_B][(r - R_A)^2 - R_B])^7} \tag{7}$$

and the polynomials $P_{2n}(R_A, R_B)$ are given in the Appendix. The longer-range attractive term $V_6(r, R_A, R_B)$ is given by the Hamaker expression[36]

$$V_6(r, R_A, R_B) = \frac{\pi^2}{3}\left[R_B\left(\frac{r - R_A}{(r - R_A)^2 - R_B^2} - \frac{r + R_A}{(r + R_A)^2 - R_B^2}\right) + \frac{1}{2}\ln\left(\frac{r^2 - (R_A + R_B)^2}{r^2 - (R_A - R_B)^2}\right) + \frac{R_B^3}{r}\left(\frac{1}{(r + R_A)^2 - R_B^2} - \frac{1}{(r - R_A)^2 - R_B^2}\right)\right] \tag{8}$$

To compute the solvent-mediated potential of mean force (PMF) between two nanocrystals, the nonlocal hypernetted chain (HNC) integral equation theory,[51,52] whose accuracy was previously ascertained for a system involving two dilute, strongly attractive LJ solutes in a supercritical LJ solvent,[42] is employed. The solution of nanocrystals is treated as a two-component mixture, with the solvent labeled as component "s" and the nanocrystals, as component "n". Within the nonlocal HNC approach, the solvent density profile induced by the two

nanocrystals is given by[42]

$$\rho(\mathbf{r}; R) = \rho_s \exp[-\beta\{u_{sn}(r) + u_{sn}(|\mathbf{r} - \mathbf{R}|) + \mu^{ex}|_{\bar{\rho}(\mathbf{r};R)} - \mu^{ex}|_{\rho_s} - (\bar{\rho}(\mathbf{r}; R) - \rho_s)\frac{\partial \mu^{ex}}{\partial \rho_s}\Big\} + \int d\mathbf{r}'\, c_s(|\mathbf{r} - \mathbf{r}'|)(\rho(\mathbf{r}'; R) - \rho_s)\Big] \quad (9)$$

where $\rho(\mathbf{r}; R)$ is the conditional probability of finding the solvent particle at $\mathbf{r}$ given that one nanocrystal is at the origin and the other nanocrystal is located at $\mathbf{R}$. In the above equation, $\beta = 1/k_BT$, $\rho_s$ is the bulk number density, $c_s(r)$ is the direct pair correlation function of the neat solvent, and $\mu^{ex}|_{\rho_s}$ is the solvent excess chemical potential evaluated at the density $\rho_s$.

The weighted local density $\bar{\rho}(\mathbf{r}; R)$ is obtained as a weighted average of the actual density profile over a microscopic volume determined by the range of the solvent pair potential:

$$\bar{\rho}(\mathbf{r}, R) = \int d\mathbf{r}' \rho(\mathbf{r}', R) w(|\mathbf{r} - \mathbf{r}'|) \quad (10)$$

$w(r)$ is the normalized weight function given by[52]

$$w(r) = \frac{\exp(-\beta u_s^{rep}(r)) - 1}{4\pi \int_0^\infty dr\, r^2 (\exp(-\beta u_s^{rep}(r)) - 1)} \quad (11)$$

with $u_s^{rep}(r) = u_s(r) + \epsilon_s$ for $r \le 2^{1/6}\sigma_s$ and $u_s^{rep}(r) = 0$ otherwise ($u_s(r)$ is the solvent−solvent LJ potential).

We remark in passing that if $\bar{\rho}(\mathbf{r}; R)$ is set equal to $\rho_s$ then eq 9 reduces to the homogeneous HNC expression for the anisotropic solvent density profile.[53] In the presence of significant solute-induced solvent density inhomogeneities characteristic of supercritical fluids,[48,49] the weighted local density deviates substantially from the bulk value, and the result for $\rho(\mathbf{r}, R)$ given by the nonlocal theory is likely to be very different from the homogeneous theory result.[42]

To solve eq 9, one needs to compute $c_s(r)$ and $\mu^{ex}$ for the neat solvent. In the present work, $c_s(r)$ is obtained by solving the Ornstein−Zernike (OZ) equation[54]

$$h_s(r) = c_s(r) + \rho_s \int d\mathbf{r}' c_s(|\mathbf{r} - \mathbf{r}'|) h_s(r') \quad (12)$$

coupled with the Percus−Yevik (PY) closure[54]

$$c_s(r) = (h_s(r) + 1)(1 - \exp[\beta u_s(r)]) \quad (13)$$

where $h_s(r)$ is the solvent total correlation function. The solvent excess chemical potential in the PY approximation is given by[55]

$$\mu^{ex} = -k_BT\rho_s \int d\mathbf{r}\, \frac{c_s(r)}{h_s(r) - c_s(r)} \ln(1 + h_s(r) - c_s(r)) \quad (14)$$

Upon substituting $c_s(r)$ and $\mu^{ex}$ from the above in eq 9, one obtains $\rho(\mathbf{r}; R)$ through an iterative procedure.

The total solute−solute PMF comprises the direct interaction potential $u_{nn}(R)$ and the excess PMF $W(R)$:

$$V(R) = u_{nn}(R) + W(R) \quad (15)$$

The excess solute−solute PMF can be calculated from the anisotropic solvent density profile via the following exact relation[55]

$$W(R) = \int_R^\infty F(R')\, dR' \quad (16)$$

where the excess mean force $F(R)$ is given by

$$F(R) = -\int d\mathbf{r}\, (\nabla u_{sn}(r) \cdot \hat{\mathbf{R}})\, \rho(\mathbf{r}; R) \quad (17)$$

The total and excess potentials of mean force are the key quantities of interest for the present study.

To solve eq 9, an iterative procedure based on the DIIS algorithm is used.[56] Using the cylindrical symmetry of the problem, anisotropic solvent density is constructed on a 2D ($r$, $\theta$) grid, and the convolution integrals in eq 9 are performed by expanding the corresponding functions in Legendre polynomials. We found that using 220 polynomials was sufficient to obtain converged results for the problems discussed in sections III and IV. The step size in the radial coordinate of the grid was taken to be 0.06 (in units of the solvent diameter), and the total number of points along this coordinate was taken to be 600.

Once the anisotropic solvent density profile was calculated, the solvent-mediated potential of mean force was obtained from eq 16, with the mean force computed from eq 17. The integral in eq 16 was calculated on a grid with a step size of 0.05 (in units of the solvent diameter).

## III. Solvophobic Case

For the purpose of presenting the results, dimensionless units defined in terms of $\sigma_s$ and $\epsilon_s$ are employed. In these units, the temperature and density are given by $T^* = k_BT/\epsilon_s$ and $\rho^* = \rho\sigma_s^3$, respectively. The calculations were performed along the supercritical isotherm $T^* = 1.41$. The critical point of the LJ fluid in the PY approximation[57] is located at $T^* = 1.291$ and $\rho^* = 0.270$, and that from simulations is located at $T^* = 1.312$ and $\rho^* = 0.316$.[58]

We first analyzed the effects of solvent density on the potential of mean force. The values of the direct interaction potential parameters were set to $\rho_c^* = 1$, $\epsilon_c^* = 5$, $\epsilon_p^* = 1$, $\epsilon_{sp}^* = 1$, $\sigma_c^* = \sigma_p^* = 1$, and $R_c^* = 3.5$ (this radius corresponds to a diameter of ∼28 Å, provided the solvent diameter is around 4 Å) for both nanocrystals. The above parameters correspond to the situation where the solute−solvent potential well depth is more shallow than the solvent−solvent well depth (solvophobic case or "repulsive" solute in the terminology of supercritical fluids).[48,59] Because the core is highly polarizable, we chose $\epsilon_c$ to be significantly larger than the values of $\epsilon_p$ and $\epsilon_s$. In addition, the density of the particles comprising the core was chosen to mimic that of a crystalline material.

The results for the excess and total potential of mean force are shown in Figure 2 for the following three values of the solvent density: $\rho_s^* = 0.15$, $\rho_s^* = 0.25$, and $\rho_s^* = 0.4$. The density of the atoms comprising the passivation layer was $\rho_p^* = 0.2$, and the passivation radius was $R_p^* = 5.5$. The upper panel of Figure 2 shows the solvent-mediated (excess) potential of mean force, and the lower panel shows the total potential of mean force between the two nanocrystals. As the solvent density increases, the excess potential of mean force between the nanocrystals becomes more attractive. Because the direct interactions between the nanocrystals are independent of solvent density, the total potential of mean force also becomes more

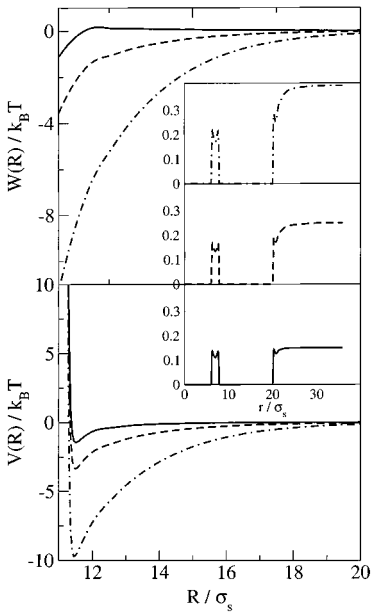


**Figure 2.** Plots of the excess potential of mean force (upper panel) and the total potential of mean force (lower panel) between solvophobic nanocrystals as a function of the separation between nanocrystals for three value of the solvent density: $\rho_s^* = 0.15$ (—), 0.25 (− − −), and 0.4 (− · −). The remaining parameters are defined in the text. The inset shows the corresponding solvent densities along the line connecting the centers of the nanocrystals for a pair separation of $R/\sigma_s = 14$.

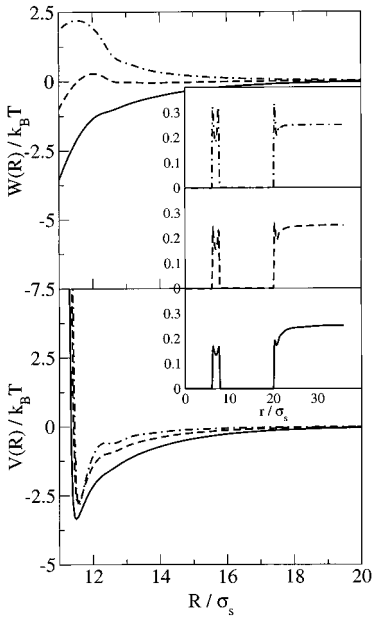


**Figure 3.** Plots of the excess potential of mean force (upper panel) and the total potential of mean force (lower panel) between solvophobic nanocrystals as a function of the separation between the nanocrystals for three values of the density of particles comprising the passivation layer: $\rho_p^* = 0.2$ (—), 0.4 (− − −), and 0.6 (− · −). The solvent density is $\rho_s^* = 0.25$, and the values of the remaining parameters are the same as those in Figure 2. The inset shows the corresponding solvent densities along the line connecting the centers of the nanocrystals for a nanocrystal−nanocrystal separation of $R/\sigma_s = 14$.

attractive as the solvent density increases. This behavior can be readily understood in terms of the local solvent density depletion around repulsive solutes at supercritical conditions,[57,59] as shown in the inset where we plot the local solvent density along the line connecting the two nanocrystals at a fixed pair separation as a function of the distance between the solvent and one of the nanocrystals ($r$). On the outside of the pair (large values of $r$), the solvent density profile is reminiscent of the profile around a single nanocrystal. The solvent density profile drops sharply to zero at values of $r$ corresponding to the locations of the two nanocrystals. The most important quantity is the density profile between the nanocrystals that is located at distances somewhat larger than the nanocrystal radius (one of the nanocrystals is located at the origin). As can be clearly seen in the Figure, the local density (relative to the bulk density) decreases with the increase of the solvent density. The relative aggregation of the solvent on the outside of the two particles, which is more favorable at larger solvent densities because of the gain in the solvent−solvent interaction energy, results in an effective attraction between them, which becomes stronger at higher densities. Therefore, we suggest that it would be easier to dissolve solvophobic nanocrystals at lower solvent densities.

Next, the effect of the density distribution of particles comprising the passivation layer (i.e. the effect of changing $\rho_p$) is analyzed. The values of the remaining parameters were set to be the same as those in the calculations presented in Figure 2, with the solvent density $\rho_s^* = 0.25$ and the passivation radius $R_p^* = 5.5$. The results are shown in Figure 3 for the following three values of the passivation density: $\rho_p^* = 0.2$, $\rho_p^* = 0.4$, and $\rho_p^* = 0.6$. The upper panel of Figure 3 shows the solvent-mediated (excess) potential of mean force between the two nanocrystals, and the lower panel shows the total potential of mean force between them. Because of the increase in the interaction strength between the solvent and the nanocrystal with increasing passivation density, the excess potential of mean force becomes more repulsive when $\rho_p$ is increased. This behavior is expected on the basis of the well-known desolvation effect, whereby a strongly interacting solute is surrounded by a relatively more dense solvation shell, which makes it more difficult to bring the two solutes into contact. This is clearly seen in the density profile shown in the inset, where the solvent density between the two nanocrystals is lower than its bulk value for the smallest value of $\rho_p$ considered, whereas it exceeds the bulk value for the largest value of $\rho_p$ considered.

The total potential, however, is largely insensitive to the density of particles in the passivation layer because the increasingly repulsive character of the excess potential of mean force is counterbalanced by the increasingly attractive character of the direct nanocrystal−nanocrystal interaction. Therefore, within the boundaries of the present model, the change in the density of the passivation layer has little effect on the desolvation of solvophobic nanocrystals. We note in passing that identical behavior is observed when one modifies $\epsilon_p$ for a fixed value of the remaining parameters, which is not surprising because changing $\rho_p$ has a similar effect on the solute−solvent interaction potential to changing $\epsilon_p$.

An additional control parameter that can be used to tune the strength of the solvent-mediated interaction between the nanocrystals is the thickness of the passivation layer, which is given by the parameter $R_p - R_c$. Given that the passivation layer in the model is composed of homogeneous LJ particles, effects such as the collapse of the passivation layer onto the core and the interdigitation of the passivating ligands are not taken explicitly into account. However, to some extent, these effects can be mapped onto our model by varying the thickness and density of the passivation layer. In a future study, we will explicitly treat the molecular nature of the passivation layer on the basis of empirical force fields.[60−62]

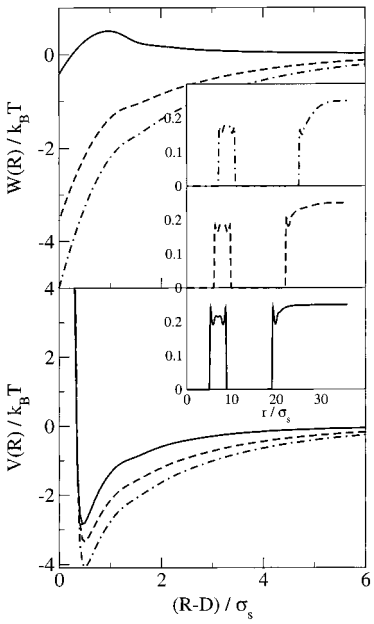


**Figure 4.** Plots of the excess potential of mean force (upper panel) and the total potential of mean force (lower panel) between solvophobic nanocrystals as a function of the separation between the nanocrystals for three values of the thickness of the passivation layer: $R_p^* = 4.5$ (—), 5.5 (− − −), and 6.5 (− · −). The parameters are defined in the text. $D = R_p^A + R_p^B$ is the average diameter of the two particles. The inset shows the corresponding solvent densities along the line connecting the centers of the nanocrystals for nanocrystal−nanocrystal separations of $R/\sigma_s = 14$, 16, and 18, respectively.

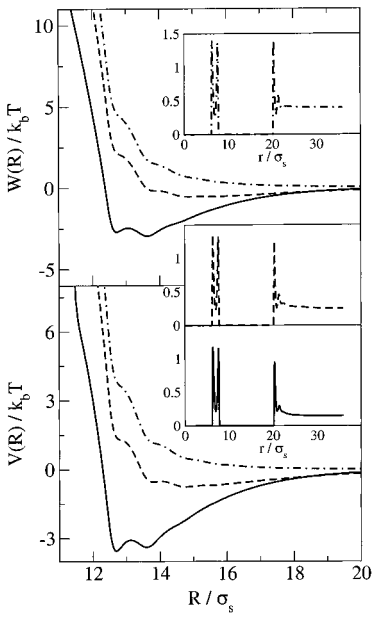


**Figure 5.** Plots of the excess potential of mean force (upper panel) and the total potential of mean force (lower panel) between solvophilic nanocrystals as a function of the separation between the nanocrystals for three values of the solvent density: $\rho_s^* = 0.15$ (—), 0.25 (− − −), and 0.4 (− · −). The remaining parameters are defined in the text. The inset shows the corresponding solvent densities along the line connecting the centers of the nanocrystals for a nanocrystal−nanocrystal separation of $R/\sigma_s = 14$.

To understand the qualitative effect of changing the thickness of the passivation layer, calculations for a fixed value of $R_c = 3.5$ at three different values of $R_p$ ($R_p^* = 4.5$, 5.5, and 6.5) were performed. The difference between two consecutive values corresponds roughly to the size of a methyl group for small-particle solvents such as $CO_2$ or $CHF_3$. The values of the remaining parameters were set to be the same as those in the calculations presented in Figure 2, with the solvent density $\rho_s^* = 0.25$ and the passivation density $\rho_p^* = 0.2$. The results for the excess potential of mean force and the total potential of mean force are shown in the upper and lower panels of Figure 4, respectively. On the basis of the behavior of the direct interaction potential between the nanocrystals (not shown), whose well depth rapidly decreases with increasing passivation thickness because of the increase in screening, one would expect that the same trend would occur in the total potential. However, the results shown in the lower panel of Figure 4 indicate that the opposite is true for solvophobic nanocrystals. A close examination of the density profiles along the direction connecting the two nanocrystals (see inset) indicates that the depletion of the solvent density around both nanocrystals increases with the radius of the nanocrystal, which results in a much more attractive solvent-mediated excess potential of mean force between the nanocrystals as the radius increases. This effect is similar to the drying of hydrophobic surfaces in water, which is more pronounced for smaller surface curvatures[63,64] (i.e., in our case, for larger nanocrystals).

## IV. Solvophilic Case

We now turn to a discussion of the solvophilic case. The values of the direct interaction potential parameters were set to $\rho_c^* = 1$, $\epsilon_c^* = 5$, $\epsilon_p^* = 1$, $\epsilon_{sp}^* = 4$, $\sigma_c^* = \sigma_p^* = 1$, and $R_c^* = 3.5$ for both nanocrystals. These parameters correspond to the situation where the solute−solvent potential well depth is more attractive than the solvent−solvent well depth (the solvophilic case or "attractive" solute in the terminology of supercritical fluids).[48,59] Note that $\epsilon_{sp}$ (the scaled interaction parameter between the solvent and the passivation layer) is the only parameter that has changed in comparison to the solvophobic case. As in the solvophobic case, the calculations were also performed along the supercritical isotherm $T^* = k_B T/\epsilon_s = 1.41$.

The results for the excess and total potential of mean force are shown in Figure 5 for the same three values of the solvent density as in the solvophobic case: $\rho_s^* = 0.15$, 0.25, and 0.4. The density of atoms comprising the passivation layer was $\rho_p^* = 0.4$ (to ensure that the solute−solvent potential well depth is more attractive than the solvent−solvent well depth), and the passivation radius was $R_p^* = 5.5$. The upper panel of Figure 5 shows the solvent-mediated (excess) potential of mean force, and the lower panel shows the total potential of mean force between the two nanocrystals. As the solvent density increases, the excess potential of mean force between the nanocrystals becomes more repulsive, in contrast to the solvophobic case. Because the direct interactions between the nanocrystals are independent of solvent density, the total potential of mean force also becomes more repulsive as the density increases. Another important difference between the solvophobic and solvophilic cases concerns the location of the minimum of the total potential, which in the present case is entirely determined by the behavior of the excess potential. Because of the strongly repulsive nature of the excess potential at the position of the minimum of the direct interaction potential, the location of the minimum corresponding to the solvent-separated stabilized pair is shifted to larger values of $R$ until the minimum in the total potential disappears at high densities. Furthermore, at the highest densities studied, the total potential is repulsive at all separations, in contrast to the solvophobic case.

The increase in the repulsion observed as the solvent density increases can be understood in terms of the local solvent density enhancement around the attractive solute at supercritical conditions, known as the clustering effect,[48,57,59] as shown in the inset. The local solvent density increases with the increase of bulk solvent density, contrary to the solvophobic case. The buildup of solvent density between the nanocrystals prevents them from forming a contact pair, which results in a more repulsive potential. However, the buildup of solvent density between the nanocrystals alone cannot explain the large changes observed in the total potential when the solvent density is varied. It is the entropy that plays the dominant role because the entropic gain in the solvent expulsion from the volume between the two nanocrystals is larger at lower solvent densities. Hence, unlike the behavior in the solvophobic case, it would be easier to dissolve solvophilic nanocrystals at higher solvent densities, as indeed was recently observed by Shah et al.[46]

We now turn to a discussion of the effect of changing the density of the atoms comprising the passivation layer on the excess and total potentials of mean force. The results are shown in Figures 6 and 7 for six values of $\rho_p$ ($\rho_p^* = 0.15$, 0.2, and 0.3 shown in Figure 6 and $\rho_p^* = 0.4$, 0.5, and 0.6 shown in Figure 7). The values of the remaining parameters were set to be the same as those in the calculations presented in Figure 5, with the solvent density $\rho_s^* = 0.25$ and the passivation radius $R_p^* = 5.5$. The upper panel in each Figure shows the solvent-mediated (excess) potential of mean force between the two nanocrystals, whereas the lower panel shows the total potential of mean force between them. The local solvent density is shown in the inset for each Figure.

Predictions made for attractive LJ particles in a LJ solvent showed that upon increasing the solute−solvent interaction strength the solvent-separated solute pair becomes anomalously stabilized at near-critical solvent conditions rather than at normal liquid conditions.[41,42] Because the effect of increasing the density of the atoms comprising the passivation layer increases the solute−solvent interactions, one would expect similar behavior for nanocrystals. However, the results shown in Figures 6 and 7 predict the opposite behavior, namely, as $\rho_p$ is increased and thus the solute−solvent interactions becomes more attractive, the excess potential of mean force becomes more repulsive, just as one would expect at normal liquid conditions because of desolvation effects. Similar behavior was observed when $\epsilon_p$ was increased.

There is a subtle difference in the features of the excess potential of mean force between the two Figures. Although all parameter values correspond to the situation where the direct solute−solvent potential is more attractive than the solvent−solvent potential, the behavior of the excess potential of mean force for the set of smaller $\rho_p$ values is reminiscent of the solvophobic case (see Figure 3). The reason that this behavior occurs can be explained by comparing the solute−solvent and solvent−solvent potentials of mean force rather than by looking at the corresponding direct interaction potentials. When the density of the passivating particles is sufficiently low, the solute−solvent potential of mean force is more shallow than the solvent−solvent potential of mean force, which leads to solvophobic-like behavior of the excess solute−solute potential of mean force.

To understand the effects of changing the thickness of the passivation layer for the solvophilic case, calculations for a fixed value of $R_c = 3.5$ at three different values of $R_p$ ($R_p^* = 4.5$, 5.5, and 6.5) were perfomred. The values of the remaining parameters were set to be the same as those in the calculations presented in Figure 5, with the solvent density $\rho_s^* = 0.25$ and the passivation density $\rho_p^* = 0.4$. The results for the excess potential of mean force and the total potential of mean force are shown in the upper and lower panels of Figure 8,

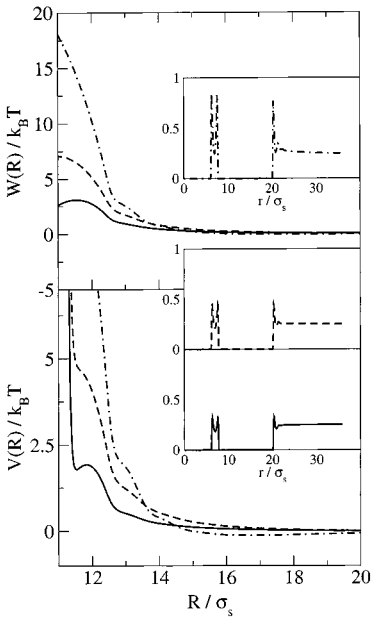


**Figure 6.** Plots of the excess potential of mean force (upper panel) and the total potential of mean force (lower panel) between solvophilic nanocrystals as a function the separation between the nanocrystals for three values of the density of particles comprising the passivation layer: $\rho_p^* = 0.15$ (—), 0.2 (− − −), and 0.3 (− · −). The solvent density is $\rho_s^* = 0.25$, and the values of the remaining parameters are the same as those in Figure 5. The inset shows the corresponding solvent densities along the line connecting the centers of the nanocrystals for a nanocrystal−nanocrystal separation of $R/\sigma_s = 14$.

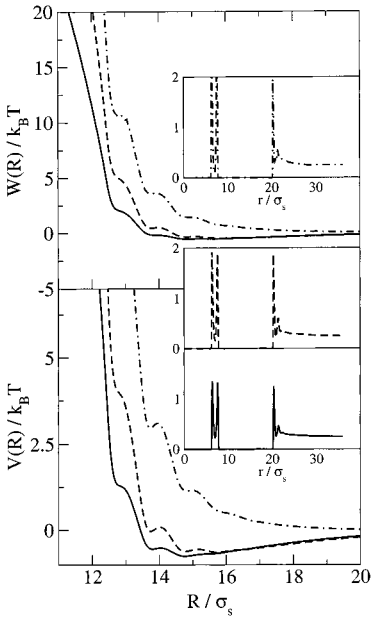


**Figure 7.** Plots of the excess potential of mean force (upper panel) and the total potential of mean force (lower panel) between solvophilic nanocrystals as a function of the separation of the nanocrystals for three values of the density of particles comprising the passivation layer: $\rho_p^* = 0.4$ (—), 0.5 (− − −), and 0.6 (− · −). The solvent density is $\rho_s^* = 0.25$, and the values of the remaining parameters are the same as those in Figure 5. The inset shows the corresponding solvent densities along the line connecting the centers of the nanocrystals for a nanocrystal−nanocrystal separation of $R/\sigma_s = 14$.

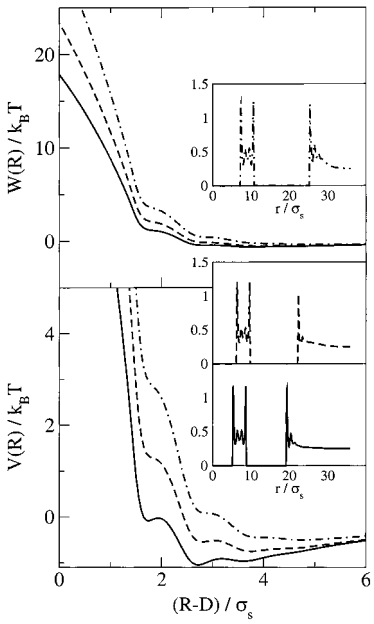


**Figure 8.** Plots of the excess potential of mean force (upper panel) and the total potential of mean force (lower panel) between solvophilic nanocrystals as a function of the separation between the nanocrystals for three values of the thickness of the passivation layer: $R_p^* = 4.5$ (—), 5.5 (− − −), and 6.5 (− · −). The parameters are defined in the text. $D = R_p^A + R_p^B$ is the average diameter of the two particles. The inset shows the corresponding solvent densities along the line connecting the centers of the nanocrystals for nanocrystal−nanocrystal separations of $R/\sigma_s = 14$, 16, and 18, respectively.

respectively. The change in the overall radius of the nanocrystals has only a slight effect on the buildup of the local solvent density (see inset), as was observed for a LJ solute in a LJ supercritical fluid.[65] This effect results in a small increase in the excess potential of mean force between the nanocrystals as the overall radius of the particles increases. Note, however, that unlike the solvophobic case the excess potential of mean force is repulsive for separations due to the aforementioned clustering effect (enhancement of local density between the nanocrystals). The well depth of the direct interaction potential decreases with increasing passivation thickness because of the screening of the highly polarizable core−core interactions. However, because the minimum observed in the total potential shifts to larger separations for the solvophilic case, the net change in the total potential is quite small. Nevertheless, one finds that it is easier to dissolve solvophilic nanocrystals as the length of the passivating ligands increases. This increased solubility was also observed experimentally for silver nanocrystals passivated with perfluorocarbons of different lengths in supercritical $CO_2$.[45]

## V. Conclusions

The excess and total potentials of mean force between nanocrystals in supercritical solvents have been calculated by using a nonlocal integral equation theory for the solvophobic and solvophilic cases. The results were analyzed by considering local density profiles of the solvent along the line connecting the two nanocrystals. The general trends observed for the excess and total potentials of mean force are markedly different for the two cases. Specifically, one finds that in going from the solvophobic case to the solvophilic case the location of the minimum corresponding to the stabilized solvent-separated pair shifts to larger separations.

Increasing the solvent density results in a more attractive total potential of mean force for solvophobic nanocrystals, whereas the opposite is true for solvophilic nanocrystals. This behavior was rationalized in terms of local solvent density depletion and enhancement around the nanocrystal pair for the solvophobic and solvophilic cases, respectively. It was shown that the solubility of solvophobic nanocrystals increases at lower solvent densities, whereas for solvophilic nanocrystals it increases at higher solvent densities. The latter conclusion is in agreement with recent experimental results on nanocrystals in supercritical fluids.[46]

The effect of changing the density of atoms comprising the passivation layer and changing the LJ energy parameter of these atoms was also carefully studied. The two parameters produce similar effects; therefore, only the former has been discussed explicitly. A strong increase in the repulsive character of the excess potential of mean force for larger values of $\rho_p$ was observed. This effect was counterbalanced by an increase of the attractive character of the direct interaction potential. As a result, the total potential of mean force is largely insensitive to changes in $\rho_p$ in the solvophobic case. The solvophilic case is somewhat more complex. Studies of LJ solutes in LJ solvent revealed anomalous behavior, where the solvent-separated pair was stabilized with the increase in the solute−solvent interaction strength. Such behavior is *not* observed in the case of nanocrystals, where the excess potential of mean force increases with $\rho_p$ or with $\epsilon_p$ for most values of separation between the nanocrystals.

Finally, the effects of changing the thickness of the passivation layer were studied. A depletion of the local solvent density, similar to the drying effect observed for hydrophobic surfaces in water, was obtained for the solvophobic case. The total potential of mean force becomes somewhat more attractive as the thickness of the passivation layer increases and the overall size of the nanocrystal increases, despite the fact that the direct interaction potential between the two polarizable cores is more strongly screened. The opposite behavior is observed for the solvophilic case because of enhancement in the local solvent density around the nanocrystals. This observation is in agreement with experimental results that indicate that the solubility of nanocrystals increases with the increasing length of passivating ligands.[45]

The theory developed here should be useful in gaining a deeper understanding of the solubility of nanocrystals in supercritical fluids. In particular, its implications are important for size-selective precipitation and for controlled assembly of nanocrystals.

**Acknowledgment.** E.R. acknowledges financial support from the United States−Israel Binational Science Foundation (grant number 9900008), from the Bergman Memorial Research Grant, and from the Israeli Council of Higher Education (Alon fellowship). S.A.E. acknowledges financial support from the Jeffress Memorial Trust (grant number J-650) and the Chemistry Department of the University of Virginia.

## Appendix: Polynomials $P_{2n}(R_A, R_B)$

In this Appendix, we provide the values for the polynomials $P_{2n}(R_A, R_B)$ that determine the short-range repulsion term

$V_{12}(r, R_A, R_B)$ in eq 7:[50]

$$P_0(R_A, R_B) = 525 \quad \text{(A1)}$$

$$P_2(R_A, R_B) = -420(R_A^2 + R_B^2) \quad \text{(A2)}$$

$$P_4(R_A, R_B) = -168(25R_A^4 - 77R_A^2 R_B^2 + 25R_B^4) \quad \text{(A3)}$$

$$P_6(R_A, R_B) = 28(R_A^2 + R_B^2)(325R_A^4 - 838R_A^2 R_B^2 + 325R_B^4) \quad \text{(A4)}$$

$$P_8(R_A, R_B) = -2(2275R_A^8 + 13\,552R_A^6 R_B^2 - 38\,502R_A^4 R_B^4 + 13\,552R_A^2 R_B^6 + 2275R_B^8) \quad \text{(A5)}$$

$$P_{10}(R_A, R_B) = -4(R_A^2 + R_B^2)(875R_A^8 - 11\,844R_A^6 R_B^2 + 22\,898R_A^4 R_B^4 - 11\,844R_A^2 R_A^6 + 875R_B^8) \quad \text{(A6)}$$

$$P_{12}(R_A, R_B) = 56(R_A^2 + R_B^2)^2(70R_A^8 - 49R_A^6 R_B^2 - 762R_A^4 R_B^4 - 49R_A^2 R_A^6 + 70R_B^8) \quad \text{(A7)}$$

$$P_{14}(R_A, R_B) = -700(R_A^2 - R_B^2)^4(R_A^6 + 11R_A^4 R_B^2 + 11R_A^2 R_B^4 + R_B^6) \quad \text{(A8)}$$

$$P_{16}(R_A, R_B) = -35(R_A^2 - R_B^2)^6(5R_A^4 + 14R_A^2 R_B^2 + 5R_B^2) \quad \text{(A9)}$$

## References and Notes


(1) Steigerwald, M. L.; Brus, L. E. *Annu. Rev. Mater. Sci.* **1989**, *19*, 471.
(2) Murray, C. B.; Norris, D. J.; Bawendi, M. G. *J. Am. Chem. Soc.* **1993**, *115*, 8706.
(3) Guzelian, A. A.; Banin, U.; Kadavanich, A. V.; Peng, X.; Alivisatos, A. P. *Appl. Phys. Lett.* **1996**, *69*, 1432.
(4) Manna, L.; Scher, E. C.; Alivisatos, A. P. *J. Am. Chem. Soc.* **2000**, *122*, 12700.
(5) Puntes, V. F.; Krishnan, K. M.; Alivisatos, A. P. *Science (Washington, D.C.)* **2001**, *291*, 2115.
(6) Leff, D. V.; Brandt, L.; Heath, J. R. *Langmuir* **1996**, *12*, 4723.
(7) Murthy, S.; Bigioni, T. P.; Wang, Z. L.; Khoury, J. T.; Whetten, R. L. *Mater. Lett.* **1997**, *30*, 321.
(8) Petit, C.; Taleb, A.; Pileni, M. P. *J. Phys. Chem. B* **1999**, *103*, 1805.
(9) Mićić, O. I.; Ahrenkiel, S. P.; Bertram, D.; Nozik, A. J. *Appl. Phys. Lett.* **1999**, *75*, 478.
(10) O'Brien, S.; Brus, L. E.; Murray, C. B. *J. Am. Chem. Soc.* **2001**, *123*, 12085.
(11) Kan, S. H.; Felner, I.; Banin, U. *Isr. J. Chem.* **2001**, *41*, 55.
(12) Sun, S.; Murray, C. B. *J. Appl. Phys.* **1999**, *85*, 4325.
(13) Colvin, V. L.; Goldstein, A. N.; Alivisatos, A. P. *J. Am. Chem. Soc.* **1992**, *114*, 5221.
(14) Murray, C. B.; Kagan, C. R.; Bawendi, M. G. *Science (Washington, D.C.)* **1995**, *270*, 1335.
(15) Vossmeyer, T.; Reck, G.; Katsikas, L.; Haupt, E. T. K.; Schulz, B.; Weller, H. *Science (Washington, D.C.)* **1995**, *267*, 1476.
(16) Ohara, P. C.; Leff, D. V.; Heath, J. R.; Gelbart, W. M. *Phys. Rev. Lett.* **1995**, *75*, 3466.
(17) Andres, R. P.; Bielefeld, J. D.; Henderson, J. I.; Janes, D. B.; Kolagunta, V. R.; Kubiak, C. P.; Mahoney, W. J.; Osifchin, R. G. *Science (Washington, D.C.)* **1996**, *273*, 1690.
(18) Harfenist, S. A.; Wang, Z. L.; Alvarez, M. M.; Vezmar, I.; Whetten, R. L. *J. Phys. Chem.* **1996**, *100*, 13904.
(19) Mićić, O. I.; Jones, K. M.; Cahill, A.; Nozik, A. J. *J. Phys. Chem. B* **1998**, *102*, 9791.
(20) Korgel, B. A.; Fitzmaurice, D. *Phys. Rev. Lett.* **1998**, *80*, 3531.
(21) Korgel, B. A.; Fullam, S.; Connolly, S.; Fitzmaurice, D. *J. Phys. Chem. B* **1998**, *102*, 8379.
(22) Sear, R. P.; Chung, S. W.; Markovich, G.; Gelbart, W. M.; Heath, J. R. *Phys. Rev. E: Stat. Phys., Plasmas, Fluids, Relat. Interdiscip. Top.* **1999**, *59*, R6255.
(23) Fried, T.; Shemer, G.; Markovich, G. *Adv. Mater.* **2001**, *13*, 1158.
(24) Ge, G.; Brus, L. E. *J. Phys. Chem B* **2000**, *104*, 9573.
(25) Kinoshita, M.; Iba, S.; Kuwamoto, K.; Harada, M. *J. Chem. Phys.* **1996**, *105*, 7177.
(26) Kinoshita, M.; Iba, S. Y.; Harada, M. *J. Chem. Phys.* **1996**, *105*, 2487.
(27) Amokrane, S. *J. Chem. Phys.* **1998**, *108*, 7459.
(28) S, S. A.; Malherbe, J. G. *J. Phys.: Condens. Matter* **2001**, *13*, 7199.
(29) Chatterjee, A. P.; Schweizer, K. S. *J. Chem. Phys.* **1998**, *109*, 10464.
(30) Rzysko, W.; Pizio, O.; Sokolowski, S. *Physica A* **1999**, *273*, 241.
(31) Shinto, H.; Miyahara, M.; Higashitani, K. *J. Colloid Interface Sci.* **1999**, *29*, 79.
(32) Shinto, H.; Miyahara, M.; Higashitani, K. *Langmuir* **2000**, *16*, 3361.
(33) Lobaskin, V. A.; Pershin, V. K. *Mol. Cryst. Liq. Cryst.* **1995**, *260*, 585.
(34) Shinto, H.; Tsuji, S.; Miyahara, M.; Higashitani, K. *Langmuir* **1999**, *15*, 578.
(35) Bouaskarne, M.; Amokrane, S.; Regnaut, C. *J. Chem. Phys.* **2001**, *114*, 2442.
(36) Hamaker, H. C. *Physica* **1937**, *4*, 1058.
(37) Bargeman, D.; Van Voorst Vader, F. *J. Electroanal. Chem.* **1972**, *37*, 45.
(38) Rabani, E.; Egorov, S. *J. Chem. Phys.* **2001**, *115*, 3437.
(39) Rabani, E.; Egorov, S. *Nano Lett.* **2002**, *2*, 69.
(40) Korgel, B. A.; Fitzmaurice, D. *Phys. Rev. B* **1999**, *59*, 14191.
(41) Kuwamoto, K.; Kinoshita, M. *Mol. Phys.* **2000**, *98*, 725.
(42) Egorov, S. A.; Rabani, E. *J. Chem. Phys.* **2001**, *115*, 617.
(43) Egorov, S. A.; Rabani, E. *J. Chem. Phys.* **2002**, *116*, 8447.
(44) Shah, P. S.; Holmes, J. D.; Doty, R. C.; Johnston, K. P.; Korgel, B. A. *J. Am. Chem. Soc.* **2000**, *122*, 4245.
(45) Shah, P. S.; Husain, S.; Johnston, K. P.; Korgel, B. A. *J. Phys. Chem. B* **2001**, *105*, 9433.
(46) Shah, P. S.; Holmes, J. D.; Johnston, K. P.; Korgel, B. A. *J. Phys. Chem. B*, in press.
(47) Ziegler, K. J.; Doty, R. C.; Johnston, K. P.; Korgel, B. A. *J. Am. Chem. Soc.* **2001**, *123*, 7797.
(48) Tucker, S. C. *Chem. Rev.* **1999**, *99*, 391.
(49) Song, W.; Biswas, R.; Maroncelli, M. *J. Phys. Chem. A* **2000**, *104*, 6924.
(50) Henderson, D.; Duh, D. M.; Chu, X.; Wasan, D. *J. Colloid Interface Sci.* **1997**, *185*, 265.
(51) Zhou, Y.; Stell, G. *J. Chem. Phys.* **1990**, *92*, 5533.
(52) Zhou, Y.; Stell, G. *J. Chem. Phys.* **1990**, *92*, 5544.
(53) Sánchez-Sánchez, J. E.; Lozada-Cassou, M. *Chem. Phys. Lett.* **1992**, *190*, 202.
(54) Hansen, J. P.; McDonald, I. R. *Theory of Simple Liquids;* Academic Press: London, 1986.
(55) Attard, P. *J. Chem. Phys.* **1991**, *94*, 2370.
(56) Kovalenko, A.; Ten-No, S.; Hirata, F. *J. Comput. Chem.* **1999**, *20*, 928.
(57) Wu, R. S.; Lee, L. L.; Cochran, H. D. *Ind. Eng. Chem. Res.* **1990**, *29*, 977.
(58) Potoff, J. J.; Panagiotopoulos, A. Z. *J. Chem. Phys.* **1998**, *109*, 10914.
(59) Chialvo, A. A.; Debenedetti, P. G. *Ind. Eng. Chem. Res.* **1992**, *31*, 1391.
(60) Luedtke, W. D.; Landman, U. *J. Phys. Chem.* **1996**, *100*, 13323.
(61) Rabani, E. *J. Chem. Phys.* **2001**, *115*, 1493.
(62) Rabani, E. *J. Chem. Phys* **2002**, *116*, 258.
(63) Lum, K.; Chandler, D.; Weeks, J. D. *J. Phys. Chem. B* **1999**, *103*, 4570.
(64) Huang, D. M.; Chandler, D. *J. Phys. Chem. B* **2002**, *106*, 2047.
(65) Egorov, S. A. *J. Chem. Phys.* **2000**, *112*, 7138.